Journal of Luminescence 204 (2018) 216–220

Contents lists available at ScienceDirect

Journal of Luminescence

journal homepage: www.elsevier.com/locate/jlumin

Influence of gold nanoparticles on the properties of stimulated emission of 6-amino-1h-phenalen-1-one in the pores of anodized aluminum oxide

A.K. Aimukhanov, N. Kh. Ibrayev

E.A. Buketov Karaganda State University, Karaganda, Kazakhstan

ARTICLE INFO

Keywords:
Dye 6-Amino-1H-phenalen-1-one (Ph160)
Plasmon resonance
Stimulated emission
Porous aluminum oxide (PAO)
Absorption and fluorescence spectra
Fluorescence kinetics
Stimulated emission threshold
Q-factor of the resonator
Gold nanoparticles (AuNPs)

ABSTRACT

The properties of stimulated emission of Ph160 dye in the pores of PAO were studied. The quantum yield of fluorescence was $F_f = 0.73$. Stimulated emission of Ph160 molecules in the pores of alumina was obtained at the maximum of fluorescence band. The threshold of stimulated emission was 1.7 MW/cm^2. It is shown that low-Q generation of stimulated emission in the film $Q \geq 1 * 10^2$ relates to the fact that the ray geometry of in the pores is not approximate to the ray geometry for the case of total internal reflection, resulting in the increase of radiative losses. The presence of gold nanoparticles in PAO results in the increase in fluorescence intensity and lowering of the generation threshold of dye stimulated emission.

1. Introduction

Cylindrical microresonators in the optical range due to the effect of total internal electromagnetic wave reflection from the walls, can support high-Q modes (~ 10^5–10^9) [1]. Since the concentration of the electromagnetic field within the cavity reaches high values, the intensity of optical transitions is greatly enhanced. For this reason, cylindrical microresonators can be used to amplify radiative transitions [2].

The actual task is to increase the output energy and frequency of repetition of laser pulses, but a number of factors prevent this. One of them is the thermal strength of the active elements, and the second is the thermal optical distortion in the active medium [3,4]. Thermo-optical distortions are observed at a temperature gradient much lower than the thermal destruction threshold of the active element and have a significant effect on the output characteristics of the laser. Thermally induced effects have a significant effect on increasing the divergence of the output laser radiation, and the thermooptical inhomogeneities manifested in the active element at high pump energies lead to a decrease in the generation efficiency [5,6].

In this aspect, porous alumina is one of the promising materials on the basis of which laser active media can be created and the structure of porous alumina represents a system of ordered pores with close packing [7]. Cavities of the cylindrical resonators can be filled with organic dye molecules having broadband fluorescence with a high quantum luminescence yield [8–10].

Membranes of anodic aluminum oxide are a promising material for the creation of high-tech devices operating at elevated temperatures [11]. The coefficient of thermal conductivity of alumina films is 1.6 W/m/K, which is much higher than the thermal conductivity of polymeric materials and glasses used as solid-state matrices in tunable dye lasers [12–14]. If pores are filled with laser dyes, then such system can be used as an active medium for a tunable laser.

For the first time the generation of stimulated emission was obtained in the pores of anodized aluminum oxide filled with rhodamine 6Zh molecules [15,16]. And follow-up studies in this direction were carried out in [17]. The present work is continuation of the studies dedicated to generation of dye stimulated emission in porous alumina. The Ph 160 dye was chosen as an active medium.

An effective and photo-stable laser dye generating radiation in the red spectral region is important for medical applications and performance indicator of the generation is comparable with the performance indicator of xanthene as well as it demonstrates generation efficiency and photo stability upon UV stimulation.

A special interest in this type of dye is conditioned by the fact that it is well luminesced in ethanol solutions and polymer matrices, and the efficiency of generation are not inferior to xanthene and pyrromethene dyes [18–20].

2. Material and methods

Synthesis of PAO was carried out according to the procedure

E-mail address: niazibrayev@mail.ru (N.K. Ibrayev).

https://doi.org/10.1016/j.jlumin.2018.08.030
Received 26 April 2018; Received in revised form 3 August 2018; Accepted 6 August 2018
Available online 08 August 2018

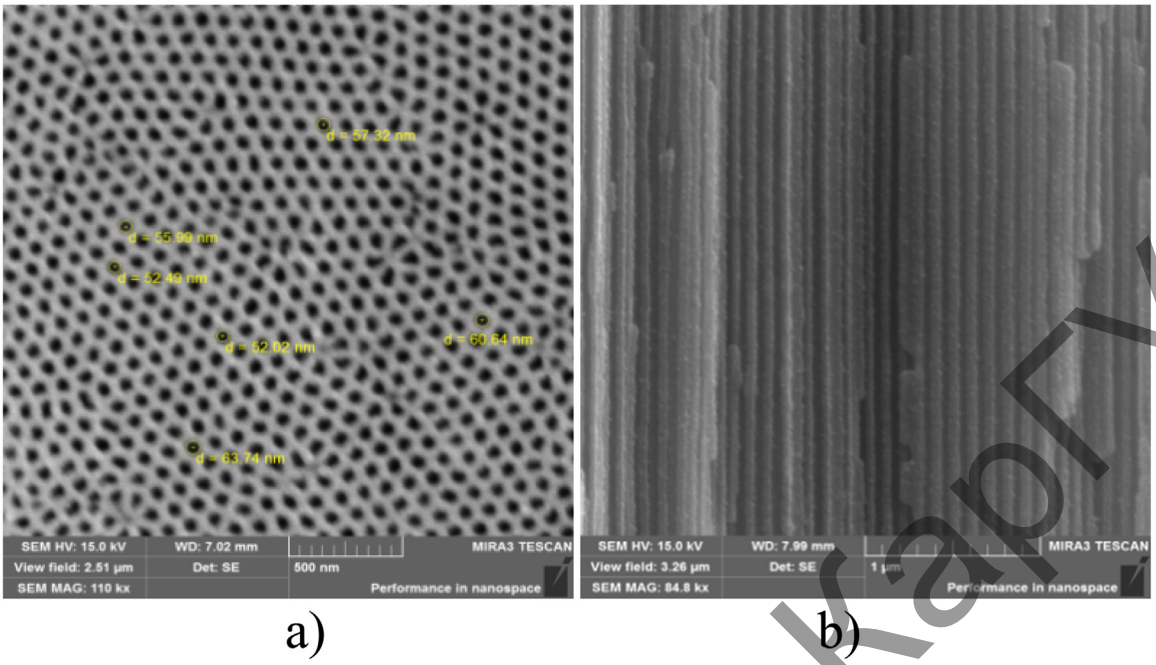

Fig. 1. SEM image of the surface (a) and the transverse cleavage of the porous film.

described in [21]. The porous aluminum oxide matrices obtained were separated from aluminum base by selective dissolution of the latter in a solution of $CuCl_2$ in HCl. A snapshot of the surface and transverse cleavage of the film obtained with a scanning electron microscope MIRA 3LMU is shown (Fig. 1). The measurements were carried out at an accelerating voltage of 7 kV, at working distance of 7 mm in a high vacuum. On the surface of the film, the pores of the same diameter were observed ~ 60 nm and with a pore distance of about 80 nm.

For the synthesis of AuNPs in the pores of anodized alumina, the following procedure was used: to the 1 ml of a working solution of $HAuCl_4$, the 9 ml of the deionized water was added in order to prepare a solution of $HAuCl_4$ of low concentration (pH 1.5–1.95).

A NaOH solution of 1 N concentration was prepared. To synthesize AuNPs in POA, the pH of the gold solution was adjusted to 10, adding the solution of NaOH (1 n). After that, a porous aluminum oxide film was immersed into the solution of $HAuCl_4$ (pH = 10) and heated at the temperature of 80 °C for 2 h. At the end of the heating process, the film acquired a crimson-pink color. This indicated the formation of gold nanoparticles in the pores. An energy dispersive analysis of the sample (Fig. 2) showed that as a result of the synthesis, the gold nanoparticles were formed on the surface and on the walls of the pores.

The sorption of dye molecules Ph160 (Fig. 3) in the pores was carried out by keeping alumina films in the ethanol solution of phosphor with initial concentration C ' = 10^{-4} mol/l for 20 h, followed by drying the films at the temperature of 100 °C for 3 h. The number of adsorbed phosphor molecules was determined according to the change

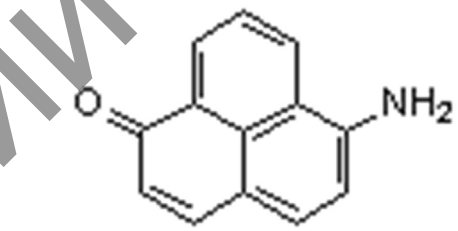

Fig. 3. The structural formula of 6-Amino-1H-phenalen-1-one (Ph160).

in the optical density of the solution before and after sorption using the equation below:

$$C = \frac{N_A * C' * V}{M * S}(1 - D_2/D_1)$$

where V is the volume of the solution, C 'is the concentration of the dye solution, D_1 and D_2 are the optical densities of the solution before and after sorption, S is the specific surface area of the porous alumina, N_A is the Avogadro number ($6.022 * 10^{23}$ mol^{-1}), M is the molar mass dye (195.22 g/mol).

3. Results and discussion

The absorption spectra of the films were measured using a Cary UV–VIS spectrophotometer (Agilent Technologies), and the fluorescence spectra were measured using Cary Eclipse (Agilent Technologies).

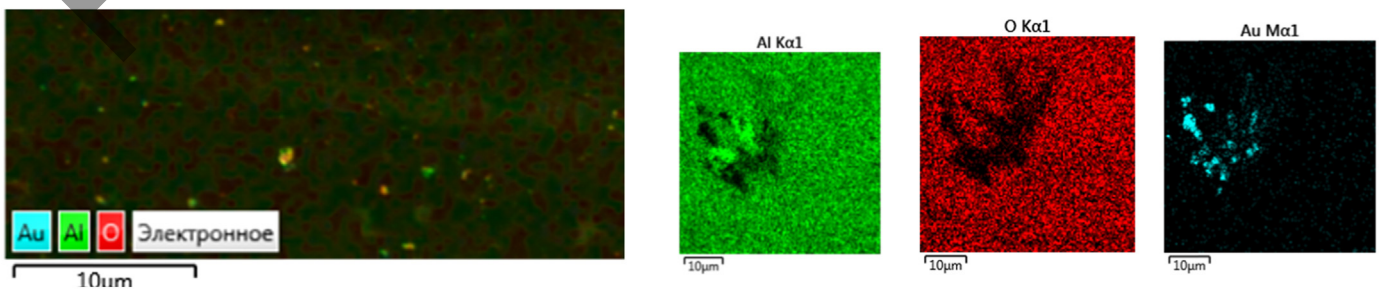

Fig. 2. Results of energy dispersive analysis of a porous film.

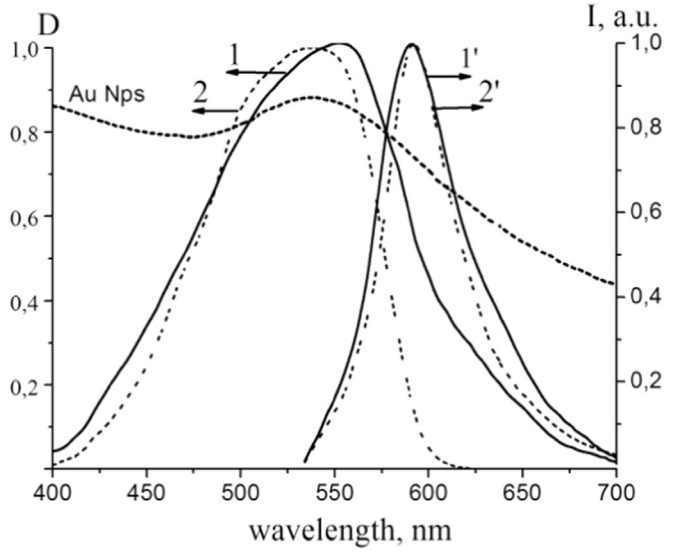

Fig. 4. Absorption spectra (1.2) and fluorescence (1 ', 2′) of the Ph160 matrix of PAO (1, 1 ') and in ethyl alcohol (2, 2′).

The photoexcitation of fluorescence of Ph160 in the PAO film was carried out at the wavelength of $\lambda = 520$ nm. The absorption and fluorescence spectra of the Ph160 molecules implanted in the channels of the porous matrix showed that the dye absorption band in the matrix had a maximum at the wavelength of $\lambda = 550$ nm (Fig. 4).

The same figure shows the absorption and fluorescence spectra of the dye molecules in the solution of ethyl alcohol at the concentration of $C = 10^{-5}$ mol/l. The dye absorption spectrum in the pores of PAO is broadened in comparison with the absorption spectrum in the ethyl alcohol, and the maximum of the spectrum is shifted to the long-wavelength region at 12 nm.

The shape of the dye fluorescence spectrum in the pores did not change compared with the alcohol solution and the positions of the spectrum maxima did not shift relative to each other ($\lambda_{max} = 591.5$ nm). As the dye molecules in the pores are densely packed, the changes in the absorption spectrum observed in comparison with alcohol solution indicate a small fraction of aggregate type of dye molecules formed. In the pores of alumina, the quantum yield of fluorescence of Ph160 molecules, determined according to the procedure [22], was $F_f = 0.73$.

The absorption spectrum of AuNPs in the PAO matrix (Fig. 4) is a wide band with the maximum at 530 nm and overlaps well with the absorption and fluorescence spectra of Ph160, indicating that the resonance conditions between the AuNPs and dye spectra are met.

The fluorescence of the dye in porous alumina with AuNPs depends on the concentration of AuNPs (Fig. 5). The luminescence intensity increases up to the concentration of $C_{Au} = 10^{-5}$ mol/l, and a further increase in C_{Au} results in quenching of the fluorescence.

According to [23,24], the reason for the enhancement of fluorescence of molecules near low-frequency metals is an increase in the rate of excitation of fluorescence due to localized plasmon resonance. At the same time, when molecules are located near a metal surface or in contact with it, non-radiative energy transfer occurs from molecules to nanoparticles resulting in the decrease in the probability of radiative decay of excited molecules.

At low concentrations of AuNPs, when nanoparticles and dye molecules are sufficiently far apart, the observed increase in fluorescence intensity of Ph160 is associated with plasmon resonance of gold nanoparticles. At high concentrations of nanoparticles, due to the decrease in the distance between fluorophores and nanoparticles, non-radiative deactivation of the excited fluorescent state of the dye dominates. Intensity of fluorescence in solutions with gold nanoparticles can

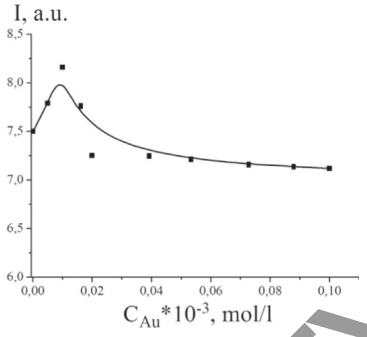

1 - 0; 2 - $2*10^{-6}$ mol / l; 3-10^{-5} mol / l; 4 - $2*10^{-4}$ mol / l.

Fig. 5. Dependence of fluorescence intensity of the dye on the concentration of AuNPs.

also increase as a result of additional absorption by dye molecules of excitation radiation scattered by nanoparticles. However, at high concentrations of nanoparticles, a non-radiative channel of decay of the excited molecules is apparently determining.

Kinetics of fluorescence of the dye was measured using a pulsed spectrometer with picoseconds resolution and recording in the time-correlated photon counting mode of Becker & Hickl. Excitation of fluorescence of the samples was carried out using a pulsed semiconductor laser with the $\lambda_{gen} = 488$ nm generation wavelength with a pulse duration at the half-height $\tau = 40$ ps.

The kinetics of fluorescence decay of Ph160 molecules in the solution (1), the porous alumina film (2), and the PAO film with gold nanoparticles (3) is shown in Fig. 6. The measurements of the kinetic fluorescence characteristics showed that the fluorescence decay of Ph160 in the solution occurred exponentially with the excited- state lifetime $\tau_{fl} = 8$ ns. The kinetics of Ph160 in PAO had non-exponential decay (Fig. 6). Analysis of the decay kinetics in a specialized program SP image 3.9.4 showed that it can be broken down into three exponents with different exponents (Table 1).

The excited state lifetime calculated from the exponential part of the decay curve of Ph160 in PAO, was 0.6 ns. When gold nanoparticles were added to the POA, the fluorescence lifetime is reduced by $\tau_{fl} = 0.4$ ns.

Measurement of spectral-energy and kinetic characteristics of the stimulated emission of PAO doped with dye molecules was carried out on the apparatus described in [11].

The spectra of stimulated emission of Ph160 molecules in a

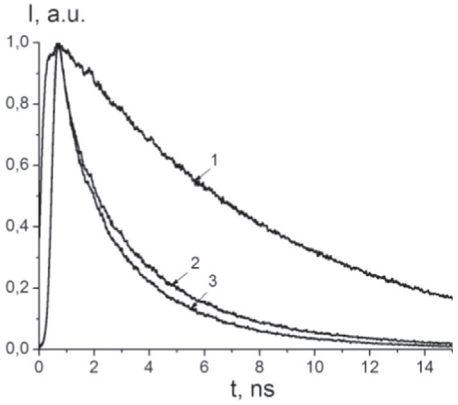

1-solution; 2- PAO; 3- PAO with AuNPs ($C = 10^{-5}$ mol / l)

Fig. 6. Ph160 Fluorescence decay kinetics.

Table 1
Influence of gold nanoparticles on the fluorescence kinetics of Ph160 in PAO.

Sample	τ_1, ps	A_1, %	τ_2, ps	A_2, %	τ_3,ps	A_3, %
Ph160 in PAO	20	85.65	1465	7.76	4499	6.59
Ph160 in PAO with AuNPs	27	26.68	1197	13.43	3589	11.36

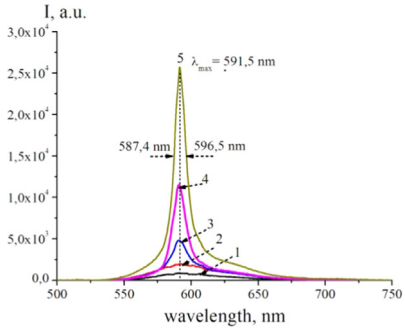

1 P = 0.5 MW / cm^2; 2 P = 1 MW / cm^2; 3
P = 2 MW / cm^2; 4 P = 3,6 MW / cm^2; 5 P = 6 MW / cm^2

Fig. 7. Spectra of Ph160 molecules generation in PAO at the different pump power densities.

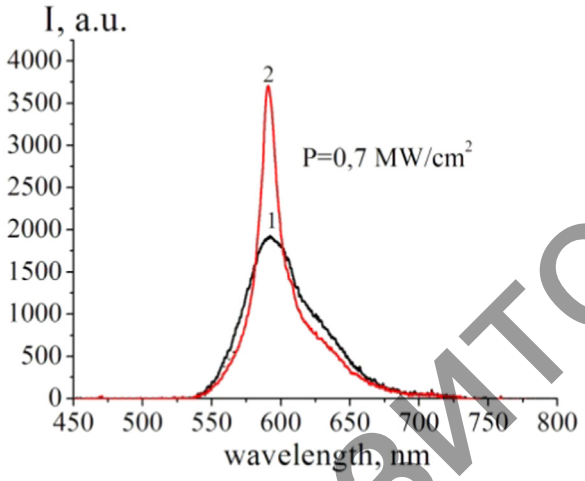

Fig. 8. Influence of AuNPs on the stimulated emission spectrum of Ph160 molecules in PAO.

cylindrical nanoresonator with a diameter D = 60 nm are shown in Fig. 7. The maximum of the induced emission of dye molecules in the film is observed at the wavelength of the fluorescence spectrum maximum. At the pump power density of up to 0.5 MW/cm^2, only a laser-induced fluorescence spectrum of the studied was observed (curve 1).

When the pump power is of the order of 1.7 MW/cm^2, a narrow band with the maximum at the wavelength of 591.5 nm (curve 3) appears on the background of the laser-induced fluorescence spectrum (curve 3), which belongs to the laser emission generation band. A further increase in the power density of the pump source results in narrowing of the fluorescence spectrum and the development of the lasing band. It is not possible to completely eliminate the component of spontaneous emission. A Q-factor of the resonator was estimated using the formula:

$$Q = \frac{\lambda}{\delta\lambda_{1/2}}$$

For the value of $\delta\lambda$ = 12 nm at the wavelength of 591.5 nm, we obtain Q ≥ 1 * 10^2. Such low-quality generation of stimulated emission

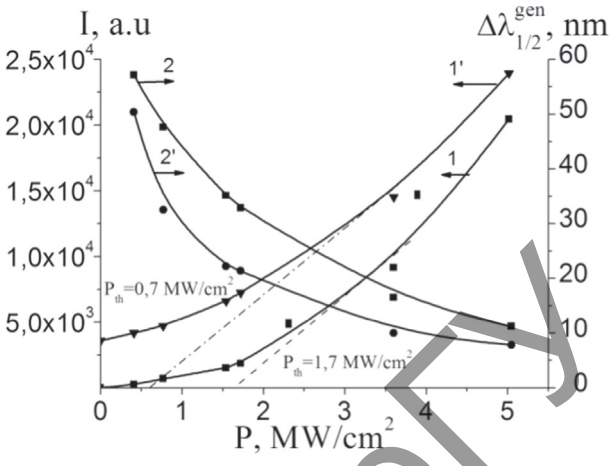

1, 2 - without AuNPs; 1', 2'-with AuNPs.

Fig. 9. Dependence of the half-width of generation line and luminescence intensity of Ph160 in the porous of PAO on the pump power density.

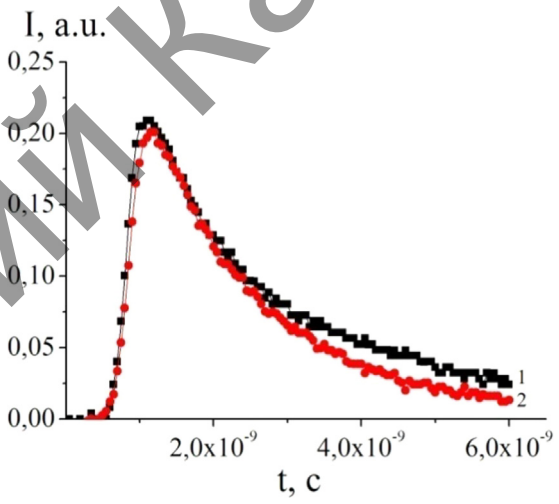

1-Ph160; 2- Ph160 with AuNPs

Fig. 10. Kinetics of stimulated luminescence of Ph160 molecules in PAO.

is due to the fact that in the case of a cylindrical resonator on a nanometer scale, ray geometry in the pores is not approximate to ray geometry for the case of total internal reflection, and as a result, radiative losses increase [1].

The effect of gold nanoparticles on the spectra of generation of stimulated emission in a PAO is shown in Fig. 8. Only the spontaneous fluorescence spectrum of Ph160 (curve 1) is observed in the PAO film at the pump power of P = 0.7 MW/cm^2.

When the pump power density is below the threshold value and equal to P = 0.7 MW/cm^2, the spectrum of stimulated emission of the dye in PAO is observed in samples AuNPs (Fig. 8, curve 2).

Based on the emission spectra measured, the half-widths of generation spectrum and intensity of the stimulated emission of the film were plotted against pump power density (Fig. 9) and film pumping thresholds were determined.

Narrowing of the radiation band with increasing excitation intensity indicates the predominance of stimulated emission over the spontaneous emission, that is, transition of the system to a generation regime. The value of the lasing threshold was determined based on a sharp change in the growth rate of radiation intensity of the film. The lasing threshold at the laser pumping λ_{gen} = 532 nm is averaged at 1.7 MW/cm^2 (Fig. 9).

Table 2
Generation characteristics of Ph160 in a porous film of PAO.

Dye	λ_{abs}^{max}, nm	λ_{fl}^{max}, nm	τ_{fl}, ns	Φ_f	τ_{gen}, ns	λ_{gen}^{max}, nm	$\Delta\lambda_{1/2}^{gen}$, nm	Generation threshold, MW / cm^2
Ph160	550	591.5	0.6	0.73	6.2	591.5	11	1.7
Ph160 + AuNPs	550	591.5	0.4	–	6	591.5	6	0.7

The effect of pump power density on intensity and half-width of stimulated Ph160 spectrum in PAO with gold nanoparticles is also shown in Fig. 9. For the sample with gold nanoparticles, the intensity of radiation at the spectrum maximum with a pump power density change from 0.1 to 5 MW/cm^2 has a sixfold increase while the half-width of the emission spectrum is narrowed by a factor of 2. Comparing experimental data of the sample with and without gold nanoparticles shows a correlation between changes in the radiation intensity and the half-width of the emission spectrum. From the data obtained, we see a decrease in the generation threshold in the presence of AuNPs in the pores of PAO. For a PAO with gold nanoparticles, the lasing threshold is reduced by a factor of 2.4.

Measurement of kinetics of the stimulated emission of PAO doped with PM567 molecules was done using the picosecond DET025A (Thorlabs) receiver and the DSO-X-3102A oscilloscope (Agilent Technologies). The width of temporary hardware function of the measuring system at the half-height was 0.3 ns. The measurement results of the emission kinetics of Al_2O_3 films with Ph160 molecules with additions of the gold nanoparticles are shown in Fig. 10.

It should be noted that duration of stimulated emission pulse Ph160 in the film is 6.2 ns and does not exceed the pulse length of the pump laser (LQ-215, SOLAR, τ_{imp} = 10 ns). When gold nanoparticles are introduced into the pores, the duration of the luminescence pulse is reduced to $\tau_{gen} \sim 6$ ns and the radiation velocity increases. Parameters of the stimulated emission spectra of Ph160 film in the pores of PAO are given in Table 2.

4. Conclusion

The quantum yield fluorescence of the Ph160 in the pores of PAO is $F_f = 0.73$. Stimulated emission of Ph160 in PAO was obtained at the maximum of fluorescence band. The threshold of stimulated emission generation averaged at 1.7 MW/cm^2. The low-Q generation of stimulated emission Ph160 in the film $Q \geq 1 * 10^2$ is due to the fact that the ray geometry in the pores is not approximate to the ray geometry for the case of total internal reflection, and as a result, the radiative losses have increased. The presence of AuNPs in porous alumina results in the increase in fluorescence intensity and lowering the threshold of dye stimulated emission. In pores with AuNPs, reduced pulse duration of stimulated emission is observed.

Acknowledgements

This work was supported in part by the Committee of Science of the Ministry of Education and Science of the Republic Kazakhstan (Grant No. BR05236691).

References

[1] V.B. Braginskii, M.L. Gorodetsky, V.S. Ichenko, Optical microresonators with whispering gallery modes, UFN 160 (1990) 157–159.
[2] V.V. Sherstnev, A. Krier, A.M. Monakhov, G. Hil, Infrared ring laser, Electron. Lett. 39 (2003) 916–917.
[3] S. Liu, F. Song, H. Cai, T. Li, B. Tian, Z. Wu, J. Tian, Effect of thermal lens on beam quality and mode matching in LD pumped Er-Yb-codoped phosphate glass microchip laser, J. Phys. D Appl. Phys. 41 (2008) (N 3. – Art. 035104).
[4] M. Scaggs, G. Haas, Real time monitoring of thermal lensing of a multikilowatt fiber laser optical system. in: Proceeding of SPIE. –. V. 8236. Art. 82360, 2012.
[5] D.G. Lancaster, J.M. Dawes, Thermal-lens measurement of a quasi steady-state repetitive flashlamp-pumped Cr, Tm, Ho: yag laser, Opt. Laser Technol. V. 30 (1998), pp. 103–108.
[6] D. Stucinskas, Thermal Lens Diagnostics and Mitigation in Diode End Pumped Lasers(Ph.D. dissertation), Vilnius University, 2010.
[7] J.W. Diggle, T.C. Downie, C.W. Coulding, Anodic oxide films on aluminum, Chem. Rev. 69 (1969) 365–405.
[8] Z.L. Zhang, H.R. Zheng, J. Dong, X.Q. Yan, Y. Sun, H.X. Xu, Surface enhanced fluorescence by porous alumina with nanohole arrays, Sci. China Phys. Mech. Astron. 55 (№ 5) (2012) 767–771.
[9] A. Moadhena, H. Elhouicheta, L. Nosovab, M. Oueslatia, Rhodamine B absorbed by anodic porous alumina: stokes and anti–Stokes luminescence study, J. Lumin. 126 (2007) 789–794.
[10] A. Moadhen, H. Elhouichet, L. Nosova, M. Oueslati, Efficient luminescence from rhodamine 6G absorbed by porous alumina: excitation mechanisms, Phys. Status Solidi (C.) 4 (№ 6) (2007) 2170–2174.
[11] A.V. Kukhta, G.G. Gorokh, E.E. Kolesnik, A.I. Mitkovets, M.I. Taoubi, Yu.A. Koshin, A.M. Mozalev, Nanostructured alumina as a cathode of organic light–emitting devices, Surf. Sci. 507 (2002) 593–597.
[12] T. Inada, N. Uno, T. Kato, Y. Iwamoto, Meso–porous alumina capillary tube as a support for high–temperature gas separation membranes by novel pulse sequential anodic oxidation technique, J. Mater. Res. 20 (№1) (2005) 114–120.
[13] G.V. Mayer, T.N. Kopylova, V.A. Svetlichny, Active polymer fibers with organic dyes, Quantum Electron. 37 (1) (2007) 53–59.
[14] E.T. Knobbe, B. Dunn, P.D. Fuqua, F. Nishida, Laser behavior and photostability characteristics of organic–dye doped silicate gel materials, Appl. Opt. 29 (1990) 2729–2733.
[15] N. Ibrayev, Kh, A.K. Zeinidenov, Plasmon–enhanced stimulated emission of Rhodamine 6G in nanoporous alumina, Laser Phys. Lett. 11 (№. 11) (2014) 1–4.
[16] N.Kh Ibrayev, A.K. Zeinidenov, A.K. Aimukhanov, K.S. Napolskii, Stimulated emission from aluminium anode oxide films doped with rhodamine 6G, Quantum Electron. V.45 (2014) 663–667.
[17] A.A. Starovoytov, T.A. Vartanyan, V.I. V. Belotitskii, Y.A. Kumzerov, A.A. Sysoeva, N.O. Alekseeva, V.G. Solovyev Emission of cyanine dye embedded in nanopores of anodic alumina matrix in: Proceedings of the International Conference Days on Diffraction, 2016, pp. 402–405.
[18] V.A. Svetlichny, T.N. Kopylova, Yu.P. Meshalkin, E.N. Prikhodko, Two-photon excitation of phenalemin 512 by Nd: YAG laser of nanosecond duration, Quantum Electron. (2004) 722–726 (T. 34. - №8. - P.).
[19] R.T. Kuznetsova, Spectroscopic and laser properties of photoexcited organic luminophors embedded in composite gel systems, Opt. Spectrosc. 102 (2) (2007) 241–251.
[20] S.M. Dolotov, M.F. Koldunov, Ya.V. Kravchenko, V.B. Lugovoi, A.A. Manenkov, V.A. Petukhov, E.P. Ponomarenko, G.P. Roskova, TS. Tsekhomskaya, An effective solid-state laser based on the composite nanoporous glass-polymer activated by phenalemic dyes (generation region 600-660 nm), Quantum Electron. 32 (8) (2002) 669–674.
[21] K. Nielsch, J. Choi, K. Schwirn, R.B. Wehrspohn, U. Gösele, Self–ordering regimes of porous alumina: the 10% porosity rule, Nano Lett. 2 (2002) 677–680.
[22] J.C. De Mello, H.F. Wittmann, R.H. Friend, An improved experimental determination of external photoluminescence quantum efficiency, Adv. Mater. 9 (1997) 230–232.
[23] P. Anger, P. Bharadwaj, L. Novotny, Enhancement and quenching of single–molecule fluorescence, Phys. Rev. Lett. 96 (2006) 113002–113005.
[24] J.R. Lakowicz, et al., Release of the self–quenching of fluorescence near silver metallic surfaces, Anal. Biochem. 320 (2003) 13–20.